

## The Long Form of FLIP Is an Activator of Caspase-8 at the Fas Death-inducing Signaling Complex\*

Received for publication, July 10, 2002, and in revised form, August 29, 2002  
Published, JBC Papers in Press, September 4, 2002, DOI 10.1074/jbc.M206882200

Olivier Micheau‡, Margot Thome‡, Pascal Schneider‡, Nils Holler‡, Jürg Tschopp‡§, Donald W. Nicholson¶, Christophe Briand¶, and Markus G. Grütter¶

From the ‡Institute of Biochemistry, University of Lausanne, 155 Chemin des Boveresses, CH-1066 Epalinges, Switzerland, the ¶Department of Biochemistry and Molecular Biology, Merck Frosst Centre for Therapeutic Research, Pointe-Claire-Dorval, Quebec H9R 4P8, Canada, and the §Institute of Biochemistry, University of Zürich, Winterthurerstrasse 190, CH-8057 Zürich, Switzerland

**Death receptors, such as Fas and tumor necrosis factor-related apoptosis-inducing ligand receptors, recruit Fas-associated death domain and pro-caspase-8 homodimers, which are then autoproteolytically activated. Active caspase-8 is released into the cytoplasm, where it cleaves various proteins including pro-caspase-3, resulting in apoptosis. The cellular Fas-associated death domain-like interleukin-1- $\beta$ -converting enzyme-inhibitory protein long form (FLIP<sub>L</sub>), a structural homologue of caspase-8 lacking caspase activity because of several mutations in the active site, is a potent inhibitor of death receptor-induced apoptosis. FLIP<sub>L</sub> is proposed to block caspase-8 activity by forming a proteolytically inactive heterodimer with caspase-8. In contrast, we propose that FLIP<sub>L</sub>-bound caspase-8 is an active protease. Upon heterocomplex formation, a limited caspase-8 autoprocessing occurs resulting in the generation of the p43/41 and the p12 subunits. This partially processed form but also the non-cleaved FLIP<sub>L</sub>-caspase-8 heterocomplex are proteolytically active because they both bind synthetic substrates efficiently. Moreover, FLIP<sub>L</sub> expression favors receptor-interacting kinase (RIP) processing within the Fas-signaling complex. We propose that FLIP<sub>L</sub> inhibits caspase-8 release-dependent pro-apoptotic signals, whereas the single, membrane-restricted active site of the FLIP<sub>L</sub>-caspase-8 heterocomplex is proteolytically active and acts on local substrates such as RIP.**

Apoptosis is a vital mechanism in multicellular organisms to eliminate unwanted cells during development, tissue homeostasis, and immune system function (1). Initiation and regulation of apoptosis is highly controlled through specific protein-protein interactions and by a family of proteolytic enzymes, the caspases (2, 3). One way to induce apoptosis is via death receptors, a subgroup of the tumor necrosis factor receptor superfamily (4). The death signal is transmitted through the binding of extracellular death ligands such as the Fas ligand (FasL)<sup>1</sup> to

its receptor Fas resulting in conformational changes of pre-formed receptor clusters (5). Intracellularly this change leads to the recruitment of the adaptor protein FADD (6, 7) and of the initiator caspases, caspase-8 and -10 (8, 9). Fas and FADD interact via homophilic death domain interactions, whereas FADD and the pro-caspases interact through death effector domains (DED). Ligand, receptor, adaptor protein, and caspases form the death inducing signaling complex (DISC) (10). When recruited to the DISC, pro-caspase-8 or -10 is activated through a series of proteolytic cleavage steps. Activation of pro-caspases generally involves the cleavage within the proteolytic caspase domain, resulting in active caspase comprising a large ( $\alpha$ ) and small ( $\beta$ ) subunit, as well as the removal of the N-terminal domain.

Apoptosis by death receptors is regulated at different levels of the signaling pathway. The viral caspase inhibitors CrmA and p35 block caspase-8 once it is activated and released from the membrane-bound DISC (11). FLIP is a potent inhibitor of death receptor-mediated pro-apoptotic signals, blocking the signaling pathway more upstream, before caspase-8 activation and release (12–19). Two forms, FLIP<sub>L</sub> (long form) and FLIP<sub>S</sub> (short form) have been characterized so far (20, 21), which correspond to FLIP splice variants at the mRNA level. FLIP<sub>S</sub> consists of two DEDs, whereas FLIP<sub>L</sub> has an additional C-terminal caspase domain and resembles caspase-8 in its overall structural organization. In the protease-like domain of FLIP<sub>L</sub> the catalytically active cysteine is replaced by a tyrosine rendering the molecule proteolytically inactive (20, 21).

Pro-caspase-8 and FLIP<sub>L</sub> are recruited to the DISC, where both molecules are partly processed and the cleaved intermediates remain bound to the DISC (12, 22). In a recent paper, Krueger *et al.* (23) demonstrated that FLIP<sub>L</sub> but not FLIP<sub>S</sub> or a mutant lacking the small subunit of the protease domain contributes to the first cleavage step of caspase-8. It is assumed that, in both cases, caspase-8 activity is highly impaired, rendering cells resistant to death receptor-induced apoptosis (24).

The precise physiological role of FLIP is still debated. Analysis of FLIP-deficient mice revealed not only its importance in the regulation of death receptor-induced apoptosis, but also in embryonic development (25). Cells deficient for FLIP are more susceptible to death receptor-mediated apoptosis (26), and this anti-apoptotic activity of FLIP is likely to control T cell survival (12). Moreover, high levels of FLIP lead to increased sensitivity

\* This work was supported by grants from the Swiss National Science Foundation (to P. S., J. T., and M. G.). The costs of publication of this article were defrayed in part by the payment of page charges. This article must therefore be hereby marked "advertisement" in accordance with 18 U.S.C. Section 1734 solely to indicate this fact.

§ To whom correspondence should be addressed. Tel.: 41-21-692-5738; Fax: 41-21-692-5705; E-mail: jurg.tschopp@ib.unil.ch.

<sup>1</sup> The abbreviations used are: FasL, Fas ligand; FADD, Fas-associated death domain; FLICE, FADD-like interleukin-1- $\beta$ -converting enzyme; DED, death effector domain; DISC, death-inducing signaling complex; FLIP<sub>L</sub>, cellular FLICE-inhibitory protein long form; FLIP<sub>S</sub>, cellular FLICE-inhibitory protein short form; PDB, Protein Data

Bank; zVAD-fmk, benzylxycarbonyl-Val-Ala-Asp-fluoromethylketone; r.m.s.d., root mean square deviation; RISC, receptor-induced signaling complex; DEVD-aomk, Asp-Glu-Val-Asp-[2,6-dimethyl benzoyloxy]-methyl ketone; mAb, monoclonal antibody; VSV, vesicular stomatitis virus; NF- $\kappa$ B, nuclear factor  $\kappa$ B; RIP, receptor-interacting kinase.

of T cells toward T cell receptor stimulation and result in increased synthesis of interleukin-2, probably as a result of the capacity of FLIP to activate the NF- $\kappa$ B and c-Jun N-terminal kinase signaling pathways (27, 28). These latter activities may also contribute to its effect on tumor growth (29, 30).

However, proapoptotic activities of FLIP<sub>L</sub> have also been described. Overexpression of FLIP in HEK 293T cells was reported by several groups to cause efficient cell death (15–19). The reason for this cytotoxic effect of FLIP<sub>L</sub> is presently unclear.

In this report, the pro-apoptotic activity of FLIP<sub>L</sub> was investigated in more detail. We demonstrate that FLIP<sub>L</sub> promotes the first proteolytic cleavage of pro-caspase-8 but prevents further cleavage of caspase-8. Caspase-8, when bound to FLIP<sub>L</sub>, shows proteolytic activity. We propose that FLIP<sub>L</sub> interacts with pro-caspase-8 through the DEDs and the protease domains. The existence of FLIP<sub>L</sub>-pro-caspase-8 heterodimers can explain the observed sequence of events at the DISC. Through association of the protease domains, FLIP<sub>L</sub> activates pro-caspase-8 differently compared with activation in a homodimer, resulting in a partially active protease restricted to the cell membrane. The consequences for cells are the interruption of the apoptotic pathway and the presence of a proteolytic complex, which may act on substrates localized at the DISC such as RIP.

#### EXPERIMENTAL PROCEDURES

**Cell Culture**—The 293T human embryonic kidney cell line were cultured in Dulbecco's modified Eagle's medium (Invitrogen) supplemented with 10% fetal calf serum and penicillin/streptomycin (100  $\mu$ g/ml of each) and grown in 5% CO<sub>2</sub> at 37 °C. Raji cells (Burkitt's lymphoma B cell lines) were cultured in RPMI 1640 containing 10% fetal calf serum and penicillin/streptomycin. Raji clones expressing FLIP<sub>S</sub>, FLIP<sub>L</sub>, or mock transfected were obtained and cultured as previously described (12).

**Reagents**—Soluble recombinant human soluble FLAG-FasL, Super-FasL, rat mAb anti-cFLIP (Dave II), and zVAD-fmk was purchased from Apotech Co. (San Diego, CA). Biotin-DEVD-aomk (L772,094) was a kind gift from Donald W. Nicholson (Merck Frosst Centre for Therapeutic Research, Quebec, Canada). Anti-FLAG (M2) antibody was from Sigma. Rabbit polyclonal anti-TRAF2 (C20) and anti-Fas (C20) were purchased from Santa Cruz Biotechnology (Santa Cruz, CA). Mouse mAb anti-RIP and anti-FADD were from Transduction Laboratories (Lexington, KY). Mouse mAb mouse anti-caspase-8 (IgG2b) was from MBL (Nagoya, Japan).

**DISC Analysis**—Raji cells were grown to densities between 1 and 2  $\times$  10<sup>6</sup> cells/ml in roller bottles, and 5  $\times$  10<sup>7</sup> cells/ml were treated with FasL (2  $\mu$ g/ml) in the presence or absence of cross-linking anti-FLAG (2  $\mu$ g/ml) for the indicated times. Cells were rapidly cooled by adding five volumes of ice-cold phosphate-buffered saline, lysed with 0.2% Nonidet P-40, Tris-HCl (20 mM, pH 7.4), NaCl (150 mM), 10% glycerol, and the protease inhibitor mixture (Roche Molecular Biochemicals). Cytosolic fractions were precleared with Sepharose 6B (Sigma-Aldrich) for 60 min and then incubated with protein G-coupled Sepharose beads (Amersham Biosciences) for 3 h. Beads were washed four times with lysis buffer. Proteins were resolved by SDS-PAGE and blotted onto nitrocellulose membranes. Blocked in phosphate-buffered saline containing 0.5% Tween 20 and 5% (w/v) dry milk, membranes were subsequently incubated with specific primary antibodies and revealed using horseradish peroxidase-conjugated goat anti-rabbit IgG, goat anti-rat IgG or goat anti-mouse (Jackson ImmunoResearch Laboratories, West Grove, PA) and ECL (Amersham Biosciences). Mouse monoclonal antibodies were specifically revealed by use of horseradish peroxidase-conjugated goat anti-mouse IgG1, IgG2a, and IgG2b from Southern Biotechnology Associates (Birmingham, AL).

**Receptor-induced Signaling Complex (RISC)**—Immunoprecipitation of the signaling complex associated to Fas receptor was performed taking advantage of the VSV-tagged version of FLIP (short or long) in the Raji clones. Briefly, cells were stimulated with Super-FasL (Apotech, www.apotech.com) for the indicated times and analyzed as described above, but immunoprecipitation was performed using an anti-VSV antibody.

**Biotinylation of Caspase-8**—Biotinylation of catalytically active caspase-8 associated to Fas receptor or FLIP was performed as follows.

Lysates of the various Raji clones stimulated with Fas ligand were incubated with 5  $\mu$ M biotin-DEVD-aomk for 30 min at 37 °C and subsequently processed for DISC or RISC analysis as described above, except that streptavidin beads were used for immunoprecipitation. Biotin-modified proteins were visualized by Western blot using streptavidin coupled to horseradish peroxidase.

**Sequence Alignment**—Crystal structures available in the PDB data bank (31) for caspase-1 (1BMQ (Ref. 32), 1IBC (Ref. 33), 1ICE (Ref. 34)), caspase-3 (1CP3 (Ref. 35), 1PAU (Ref. 36), 1GFW (Ref. 37)), caspase-7 (1GQF (Ref. 38), 1F1J (Ref. 39), 1I4O (40), 1I51 (Ref. 41), 1K86 (Ref. 42), 1K88 (Ref. 42), 1KMC (Ref. 38)), caspase-8 (1QDU (Ref. 43), 1QTN (Ref. 44), 1F9E (Ref. 45)), and caspase-9 (1JXQ (Ref. 46)) were used for structural alignment in the following way; all  $\alpha/\beta$  heterodimers were superimposed using the six-dimensional search algorithm implemented in the program Superimpose (47). Taking the C $\alpha$  positions of the caspase-8 structure as a reference C $\alpha$  position, differences were calculated using the program Strupro (O related program) between corresponding residues of the template and each superimposed  $\alpha/\beta$  heterodimer. Amino acids, for which the C $\alpha$  distance was less than 3.5 Å, were defined as structurally aligned residues (48). The sequence of c-FLIP<sub>L</sub> was then aligned to this structure-based sequence alignment template using ClustalX (49). Manual corrections were applied to align deletions and insertions of FLIP<sub>L</sub> with insertion and deletion regions in the template.

**Model Building**—Model structures for the FLIP<sub>L</sub> heterodimer were created using all available heterodimer structures (Modeler (Ref. 50)) and the alignment described above. Model structures for the heterotetrameric  $\alpha/\beta/\beta/\alpha$  caspase-8-FLIP<sub>L</sub> were calculated using the structure of caspase-9 (46) as a template. Model structures of the heterotetrameric  $\alpha/\beta/\beta/\alpha$  pro-caspase-8-FLIP<sub>L</sub> were computed using the structure of caspase-7 (38) as a template. Each model was checked with Procheck (CCP4 program suite (Ref. 51)) using a resolution of 3.0 Å. In each case the model with the best stereochemistry was chosen for further analysis.

**Calculation of Shape Surface Complementarity**—The shape surface complementarity of the  $\beta\beta$  interfaces of both the heterotetramer pro-caspase-8-FLIP<sub>L</sub> and caspase-8-FLIP<sub>L</sub> was calculated using the program SC from CCP4 (52). The probe sphere used to define the solvent-excluded surface was set to 1.7 Å. A peripheral band of 1.5 Å that is a part of the buried portion of the molecular surface was omitted from the calculation. A weighting factor of 0.5 Å<sup>-2</sup> was used in the calculation of the surface complementarity (52, 53). Surfaces were visualized using GRASP (54). The color ramp used in GRASP was defined as blue for a SC value of 1 going to white for a SC value of 0. Interfaces colored in blue match precisely, whereas white interface areas are not correlated. Non-interacting surfaces are colored in red.

**Calculation of Electrostatic Surface Complementarity**—Surface electrostatics were calculated using the program GRASP (54) applying charges files (full.crg and back\_no\_h.crg) and radii file (default.siz). The inner dielectric constant was set to 4.0 and the bulk salt concentration to 0.145 (55).

The electrostatic surface complementarity is illustrated by coloring the surface of both interacting subunits. Regions where the colors are opposite (blue-red for complementarity) match, whereas identical colors indicate electrostatic clashes. For simplicity the surface color of one interaction partner was projected onto the other. The desolvation potential and the bound-state potential were calculated as described by Kangas *et al.* (55).

**Calculation of r.m.s.d. Values**—r.m.s.d. values were calculated using the command lsq\_explicit from the program O (56) for C $\alpha$  positions. For this analysis, residues 322–334, 338–341, 347–360, 365–374, 387–389, and 393–401, which form the secondary structure elements in caspases (numbering from coordinate structure 1ICE (34) were used to define the central core of the  $\beta$  subunit. The r.m.s.d. values of the  $\beta$  core in the pro-caspase-8-FLIP<sub>L</sub> and the caspase-8-FLIP<sub>L</sub> model were calculated using the  $\beta$  core of caspase-8-caspase-8 as a template (PDB file 1F9E (Ref. 45)). As a negative control, the r.m.s.d. of the  $\beta$  core in a caspase-3-FLIP<sub>L</sub> model was also calculated using the  $\beta$  core of caspase-3 as a template (PDB file 1CP3 (Ref. 43)).

#### RESULTS

In agreement with several previous reports (12, 14–19), we found that FLIP<sub>L</sub>, when overexpressed at high levels in 293T human embryonic kidney cells, did not protect cells from apoptosis but efficiently caused cell death in a ligand-independent manner (Fig. 1A). In contrast to FLIP<sub>L</sub>, FLIP<sub>S</sub> caused little or no cell death (Fig. 1A). FLIP<sub>L</sub>-induced cell death was inhibited

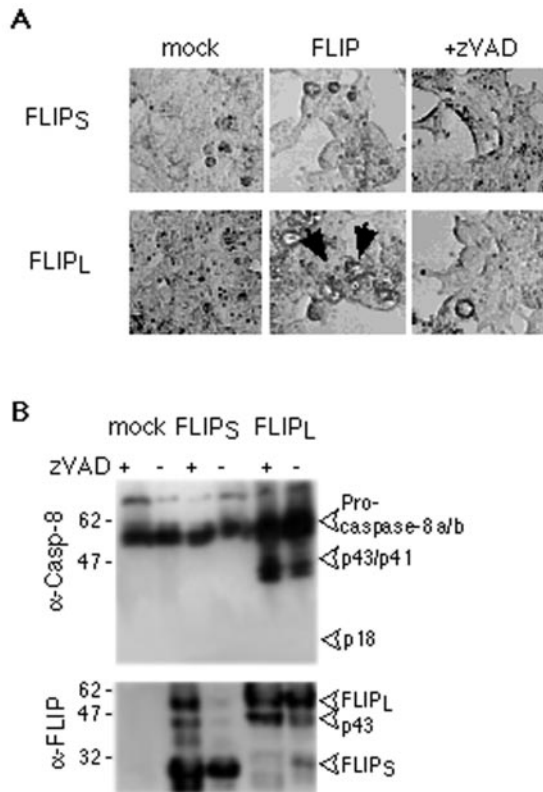


**FIG. 1. FLIP<sub>L</sub> induces apoptosis in 293T cells.** *A*, 293T cells were transfected with 5  $\mu$ g of plasmid coding for FLIP<sub>L</sub> and FLIP<sub>S</sub>, respectively (control, *mock*). Cells were analyzed by confocal microscopy. The *arrow* points to rounded, typically apoptotic cells. *B*, cell extracts were analyzed by Western blot analysis for the expression of transfected FLIP<sub>L</sub> using an  $\alpha$ -FLIP antibody and for processing of endogenous caspase-8 ( $\alpha$ -Casp-8). Note that the inhibitor zVAD-fmk does not efficiently block caspase-8 processing.

by zVAD-fmk and Ile-Glu-Thr-Asp-fluoromethylketone (Fig. 1 and data not shown), suggesting that FLIP<sub>L</sub> can induce apoptosis via activation of caspase-8. We therefore analyzed whether caspase-8 activation differed in cells expressing either FLIP<sub>L</sub> or FLIP<sub>S</sub>. Caspase-8 was indeed partially processed in cells overexpressing FLIP<sub>L</sub>, whereas, in cells harboring the small form, primarily the precursor caspase-8 was detectable (Fig. 1*B*). FLIP<sub>L</sub>-induced caspase-8 processing was dose-dependent and became apparent when cDNA doses of FLIP used for transfection were high (data not shown). Activation of caspase-8 is thought to occur in a two-step mechanism. The initial cleavage occurs after Asp-374 (Asp-299 using 1ICE numbering (Ref. 34)), giving rise to the p43/p41 and the p12 subunits, whereas, in a second step, cleavage occurs after Asp-216 and Asp-384 (Asp-143 and Asp-309 in 1ICE numbering), generating the p18 ( $\alpha$ ) and p10 ( $\beta$ ) subunits of the active enzyme (11). Interestingly, FLIP<sub>L</sub>-induced caspase-8 processing was limited to the first step, as further processing of the p43/p41 fragment was not observed. This suggested that processing between the large and small subunit suffices to expose the caspase-8 active site.

We next decided to investigate whether, upon Fas stimulation, partial caspase-8 processing also occurs in cells overexpressing FLIP<sub>L</sub> and whether the FLIP-bound activated caspase-8 exhibited proteolytic activity. To this end, DISC formation was analyzed in Raji B cells stably transfected with either FLIP<sub>L</sub> or FLIP<sub>S</sub> (Fig. 2). Recombinant, FLAG-tagged FasL was added to Raji cells and anti-FLAG immunoprecipitates analyzed after various periods of time. Rapid recruitment of FADD, RIP, caspase-8, and FLIP to the engaged receptor

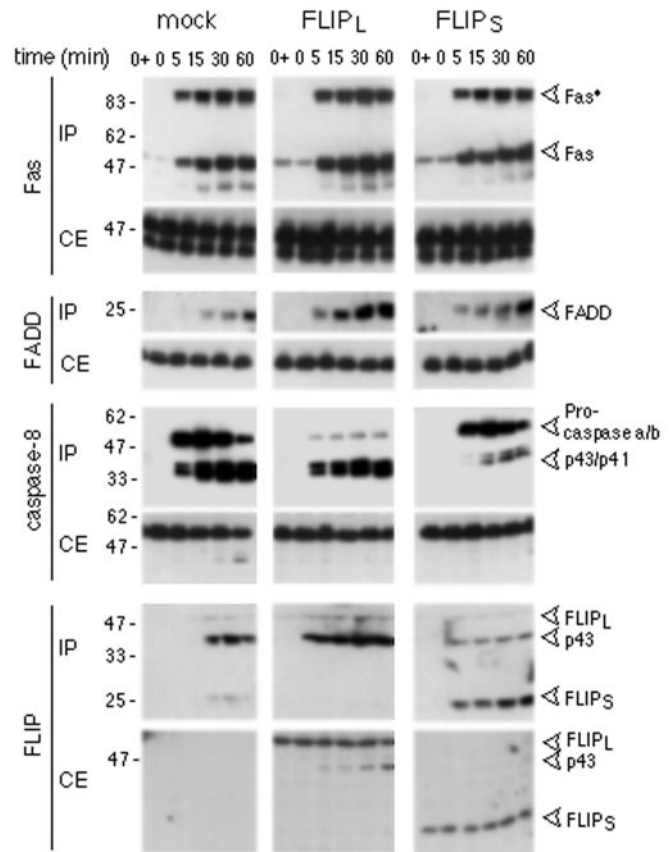


**FIG. 2. FLIP<sub>L</sub> induces processing of caspase-8.** Western blot of lysates (*CE*) and DISCs (*IP*) of Raji cells stably transfected with empty vector (*mock*), VSV-FLIP<sub>L</sub>, or VSV-FLIP<sub>S</sub>. Cells were stimulated for various time periods with FLAG-tagged FasL, which, after detergent lysis, was subsequently immunoprecipitated using the anti-FLAG M2 antibody. In time point 0+, the FasL was added after lysis. The extracts and the DISC were analyzed for the presence of Fas, FADD, caspase-8, and FLIP using the respective antibodies. *Fas\** refers to a high molecular mass species of Fas, which occurs upon FasL engagement.

was observed (Figs. 2 and 5). In cells overexpressing FLIP<sub>L</sub>, partial cleavage of caspase-8 in the DISC was most rapid. By 5 min after the addition of FasL, complete conversion of the caspase-8 precursor form into the p43/p41 partially processed form was detected in the DISC, whereas, in the cytoplasmic caspase-8 pool, no processing of caspase-8 was noticeable even 1 h after ligand addition. In contrast, in cells expressing FLIP<sub>S</sub>, most of the caspase-8 remained in the precursor form at the level of the DISC and in the cytoplasm, in accord with a previous report using BJAB B lymphoid cell (23). The p43/p41 band was also detectable in wild-type Raji cells despite the fact that wild-type Raji cells did not express detectable FLIP<sub>L</sub> in cell extracts (Fig. 2). However, closer examination revealed that endogenous processed FLIP<sub>L</sub> was enriched at the level of the DISC, which may explain the presence of partially processed caspase-8. Thus, caspase-8 processing is rapid and efficient in the presence of FLIP<sub>L</sub> but not FLIP<sub>S</sub>, indicating that the caspase-8 moiety of FLIP is required to promote partial caspase-8 processing.

If a direct interaction between FLIP<sub>L</sub> and caspase-8 induces processing of caspase-8, predominantly processed caspase-8 should be found in association with FLIP<sub>L</sub> but not with FLIP<sub>S</sub>. To test this prediction, we analyzed caspase-8 association with FLIP during DISC formation, by immunoprecipitating FLIP using antibodies recognizing the VSV-tagged transfected FLIP. In a FasL stimulation-dependent manner, FLIP immunoprecipitates contained caspase-8, FADD, and Fas (Fig. 3). A large

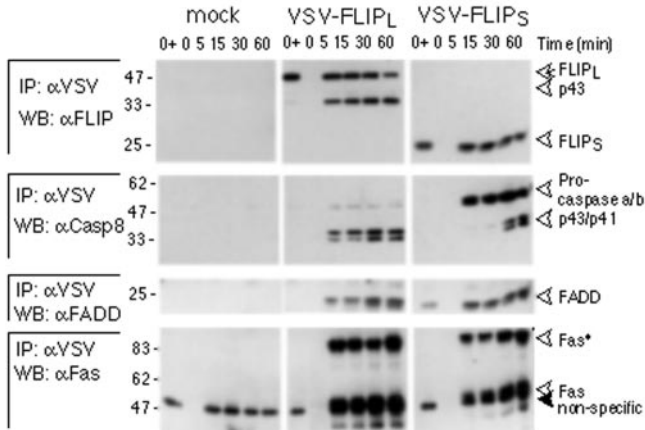


**FIG. 3. FLIP<sub>L</sub> is associated primarily with processed caspase-8.** Cells were stimulated with FLAG-tagged RISCs as in Fig. 2. Following cell lysis, VSV-tagged FLIP proteins were immunoprecipitated (IP) with an α-VSV antibody and the associated complex was analyzed by Western blot (WB). The filled arrowhead refers to a non-specific band. In time 0+, FasL was added after detergent lysis.

portion of the co-precipitated Fas migrated with a molecular mass of >120 kDa. This modified form of Fas, which most likely corresponds to aggregated Fas (10), is exclusively seen upon Fas engagement (see also Fig. 2). All caspase-8 associated with FLIP<sub>L</sub> was partially autoprocessed. In contrast, mostly pro-caspase-8 was found in FLIP<sub>S</sub> immunoprecipitates, suggesting that the conformational changes required for partial processing of caspase-8 are dependent on the caspase-like domain of FLIP.

It has been previously proposed that FLIP inhibited cell death by blocking the proteolytic activity of caspase-8 (24). However, this is incompatible with the observation that FLIP<sub>L</sub> undergoes a caspase-8-dependent rapid processing between the large (α) and small (β) subunit of the caspase domain at Asp-376 (Asp-299 in 1ICE numbering; see Figs. 1–3), resulting in the generation of the 43- and 12-kDa fragments. Because FLIP is proteolytically inactive, processing of FLIP<sub>L</sub> most likely occurs through an adjacent caspase-8.

To get more direct evidence for the enzymatic activity of FLIP-bound caspase-8, DISC-associated caspase-8 was analyzed for its capacity to interact with the biotinylated inhibitor DEVD-aomk (57). Although this inhibitor was originally designed for caspase-3, it blocks the activity of most caspases at higher concentrations.<sup>2</sup> This active-site probe requires catalytic turnover to covalently biotinylate the active site cysteine. The DISC was isolated in the presence of the biotinylated inhibitor and incorporation examined by Western blot analysis using streptavidin (Fig. 4). Two molecular species were found to be biotinylated, which corresponded in size to precursor caspase-8 a/b and to its p43/p41 partially cleaved forms (Fig. 4A). Interestingly, the presence of the caspase inhibitor during the lysis procedure significantly blocked processing resulting in an almost complete absence of the p43/p41 species. Although FLIP cleavage was reduced it was not completely abolished (Fig. 4A), suggesting that even precursor caspase-8 must have some proteolytic activity, in accord with the observation that the pro-form incorporates biotinylated substrate.

Inhibition of caspase-8 autoprocessing and biotinylation of the zymogen form of caspase-8 was also observed when the DISC was immunoprecipitated via FLIP (Fig. 4B). Surprisingly, some caspase-8 association to FLIP was found to occur already at time 0, which is in contrast to the experiments shown in Fig. 3. As the only experimental difference was the

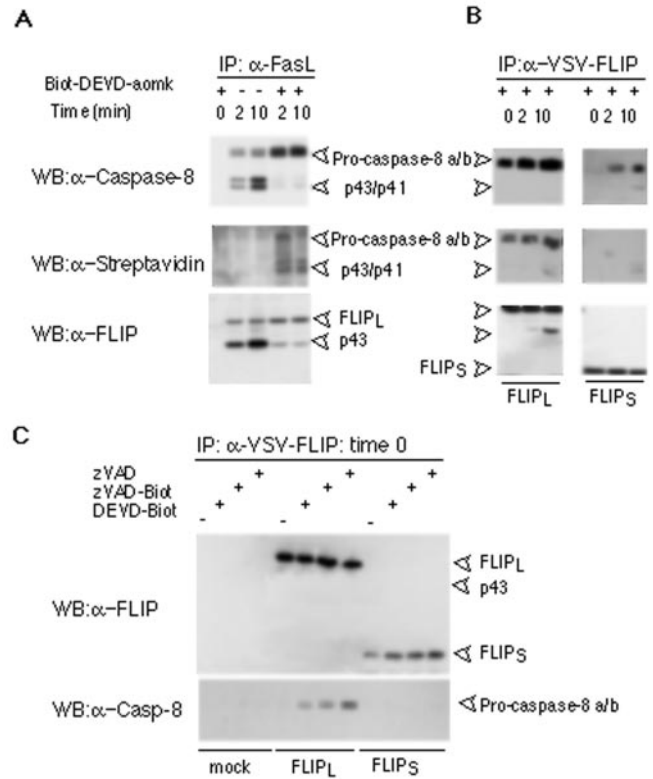


**FIG. 4. Non-processed and processed caspase-8 are proteolytically active.** A, DISC analysis of VSV-FLIP<sub>L</sub>-transfected Raji cells using FasL to immunoprecipitate (IP) the complex. After cell lysis, extracts were treated with biotin-DEVD-aomk and subsequently analyzed by Western blotting (WB) using antibodies to caspase-8 or streptavidin to detect the covalently linked caspase inhibitor. B, VSV-FLIP<sub>L</sub> and VSV-FLIP<sub>S</sub>-transfected Raji cells were treated as in A. FLIP was immunoprecipitated with α-VSV antibodies, and associated proteins analyzed by Western blot analysis. C, FLIP-associated proteins were analyzed without prior addition of FasL in the presence or absence of the indicated caspase inhibitors.

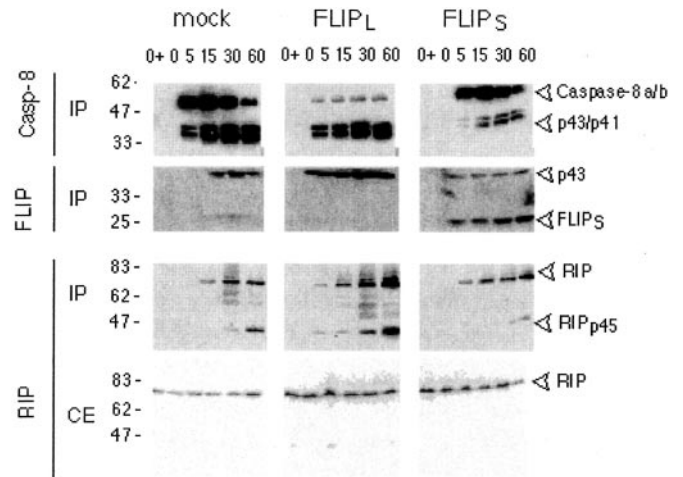


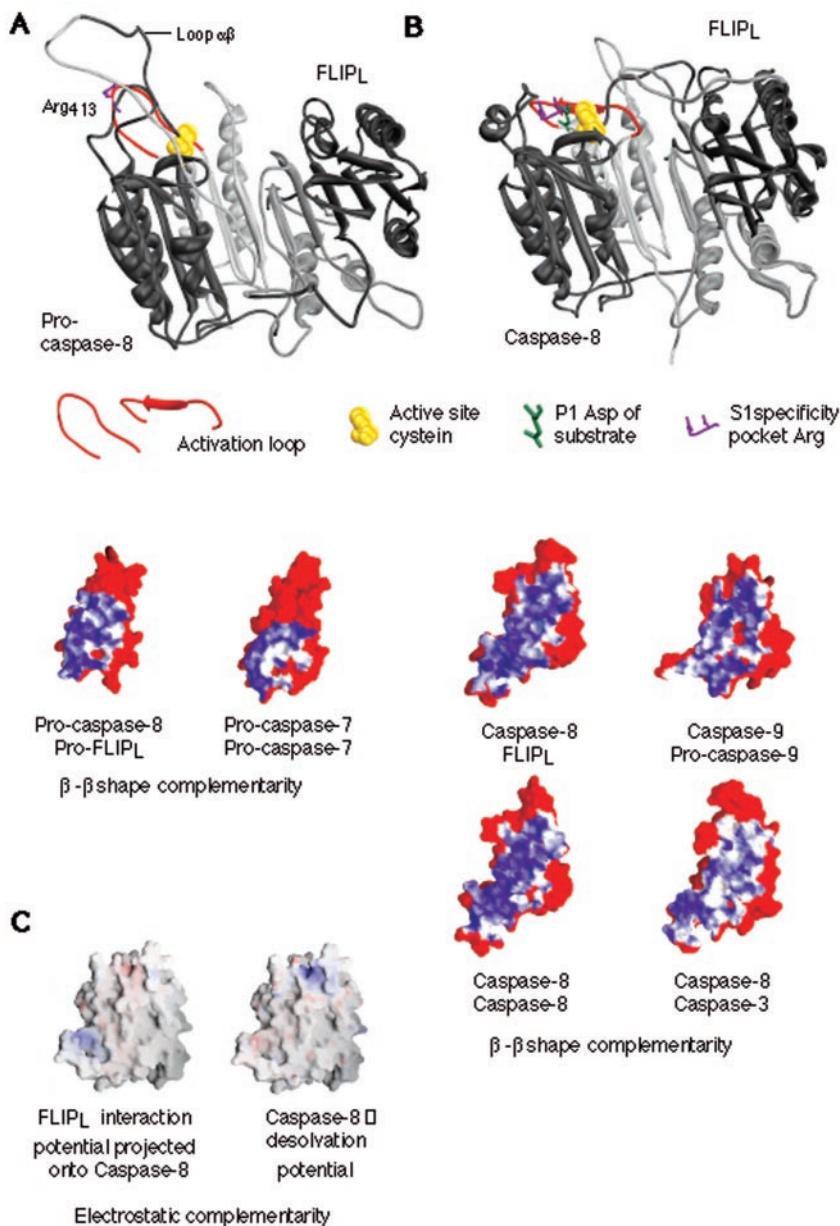
**FIG. 5. The caspase-8-FLIP<sub>L</sub>, but not the caspase-8-FLIP<sub>S</sub> heteromer induces cleavage of DISC-bound RIP.** DISC analysis is shown as described in Fig. 2. Note the appearance of cleaved RIP (RIPp45) in cells with high levels of FLIP<sub>L</sub>. Abbreviations are as in Fig. 2.

presence of caspase inhibitors, we repeated the experiments in the presence of two other caspase inhibitors, *i.e.* zVAD-fmk and biotin-zVAD-fmk. Again, FLIP-bound caspase-8 was seen without prior FasL stimulation (Fig. 4C), suggesting that binding of the inhibitor promotes association. This suggests a model in which, upon caspase-8 binding to FLIP<sub>L</sub>, non-cleaved caspase-8

<sup>2</sup> D. Nicholson, unpublished observation.



**FIG. 7. Models of caspase-8-cFLIP<sub>L</sub> hybrid molecules.** **A**, model of pro-caspase-8-FLIP<sub>L</sub>. Pro-caspase-8 (left) interacts mainly via  $\beta$ - $\beta$  contacts with FLIP<sub>L</sub> (right). The activation loop, shown in red, keeps the active site of pro-caspase-8 in an inactive conformation. Notably, Arg-413 (purple), which is part of the S1 specificity pocket for the P1 Asp residue of the substrate, is kept remote from the active site. p18 subunits (dark gray), p12 subunits (light gray), and caspase-8 active site Cys (yellow, space-filling representation) are also shown. The shape complementarity (in blue for high shape complementarity and white for low shape complementarity) of the interface is comparable with that observed in the interface in the pro-caspase-7 structure (38). **B**, model of caspase-8-FLIP<sub>L</sub>. In the caspase-8-FLIP<sub>L</sub> model, the caspase-8 active site adopts the same conformation as the one observed in the inhibited structure of caspase-8 (45). The activation loop is rearranged to create a functional active site that can accommodate the P1 Asp residue of the substrate (green). The shape complementarity of the interface is comparable with that observed in the interface in caspase-9 (46). Small cavities (red) are visible in the caspase-9 interface. The shape complementarity is very similar to the one observed in the caspase-8 interface (45). In contrast, low shape complementarity is observed in a control model showing the interface of a non-physiological caspase-8-caspase-3 hybrid molecule. **C**, electrostatic complementarity in the caspase-8-FLIP<sub>L</sub> model. The electrostatic complementarity (blue for positively charged areas and red for negatively charged areas) at the interface between caspase-8 and FLIP<sub>L</sub> is displayed. On the left side the caspase-8 surface is shown with the FLIP<sub>L</sub> interaction potential projected onto it. On the right side the surface potential of caspase-8 is displayed. Both interfaces are compatible. Pictures were drawn using Setor (67).



zymogen undergoes a conformational rearrangement, thereby acquiring catalytic competency. Binding of the inhibitor then stabilizes this interaction and blocks autoprocessing.

We wondered whether the single active site present in the FLIP<sub>L</sub>-caspase-8 heterodimer bound in the DISC would locally cleave substrates other than FLIP. We reasoned that the most likely candidates were proteins sterically close to FLIP<sub>L</sub>-caspase-8, *i.e.* components of the DISC such as Fas, FADD, and RIP. Indeed, a rapid processing of the kinase RIP was detectable (Fig. 5). A fragment of 38 kDa in size was detected immediately after RIP recruitment to Fas in cells expressing FLIP<sub>L</sub>. This corresponds in size to the fragment previously reported to be generated through caspase-8 (Refs. 58 and 59 and data not shown). Cleavage occurs at a typical caspase-8 site (LQLD<sup>324</sup>) and separates the kinase domain from the death domain. Processing was considerably reduced in cells overexpressing FLIP<sub>S</sub>, indicating that the caspase-like domain of FLIP promotes the cleavage. Moreover, RIP processing was not observed in the cytoplasm, demonstrating that RIP cleavage occurs at the level of the DISC and is not caused by caspase-8 released into the cytoplasm.

The above results suggested that a heterodimeric FLIP<sub>L</sub>-caspase-8 complex can form in the DISC displaying enzymatic activity, which does not, however, cause apoptosis. This complex is quite unique, because the described functional caspases are all thought to be homodimers. To strengthen this evidence for the existence of FLIP<sub>L</sub>-caspase-8 heterodimers, a three-dimensional model of the caspase-like domain of FLIP<sub>L</sub> was constructed, based on the alignment and on the three-dimensional structures of caspase-8, -1, -3, -6, and -7 (Fig. 6A). The resulting FLIP<sub>L</sub> model (Fig. 6B) did not contain any bad contacts in the  $\alpha/\beta$  interface and exhibited a good geometry and electrostatic complementarity. The high quality contacts in the  $\alpha/\beta$  interface are supportive for a caspase-like fold of FLIP<sub>L</sub>.

Two c-FLIP<sub>L</sub>-caspase-8 heterodimer models were subsequently created (Fig. 7A). The pro-caspase-8-FLIP<sub>L</sub> model was based on the structure of pro-caspase-7 (38), and the caspase-8-FLIP<sub>L</sub> model was based on the structure of caspase-9 (46) as a template. For both models the caspase-8-FLIP<sub>L</sub> interfaces were analyzed. Only small rearrangements in caspase-8 were needed to accommodate a FLIP<sub>L</sub> molecule (Table I).

Analysis of the interface formed between (pro-)caspase-8 and

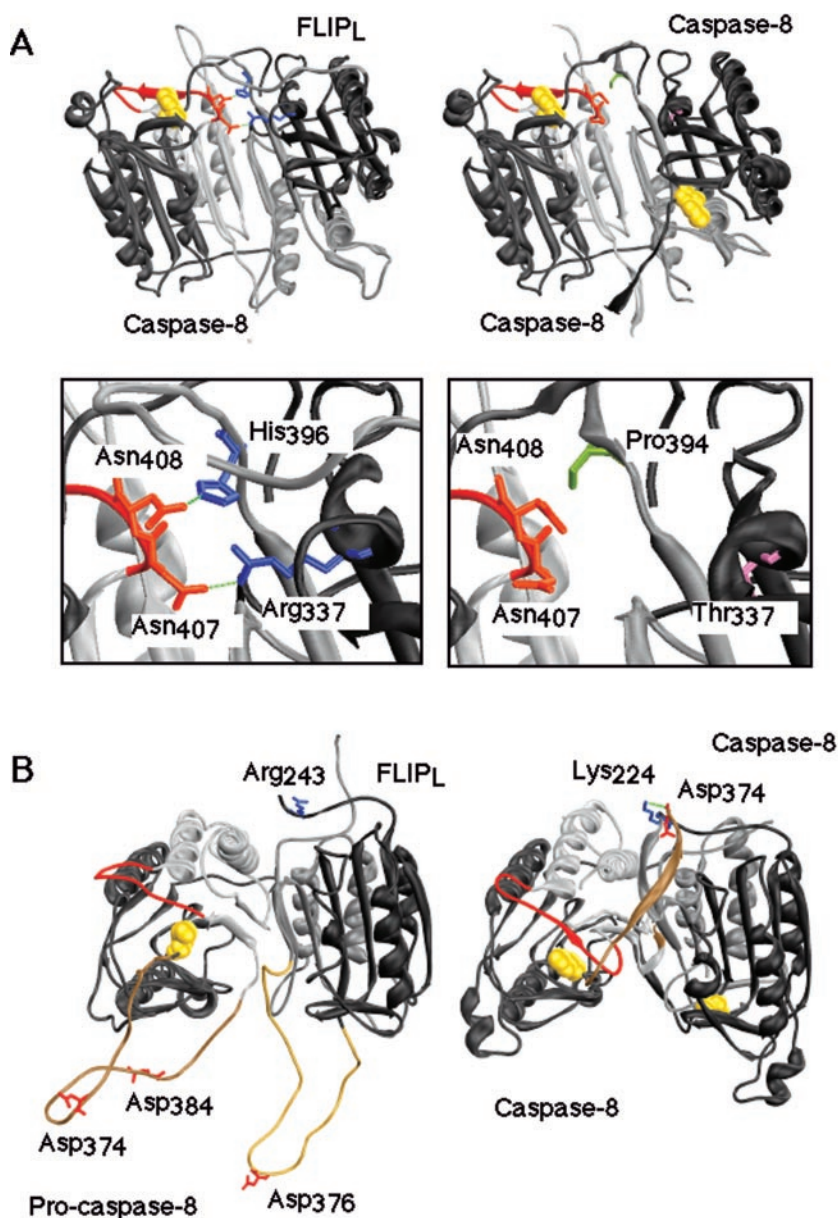
TABLE I  
*C $\alpha$*  r.m.s.d. of  $\beta$ -caspase-8 and of  $\beta$ -caspase-3 during complexation with FLIP<sub>L</sub>

In the caspase-8-FLIP<sub>L</sub> heterodimer, a small readjustment of the  $\beta$ -subunit of caspase-8 is required to accommodate  $\beta$ -FLIP<sub>L</sub>. Readjustment in the  $\beta$ -subunit of caspase-3 is larger (r.m.s.d. 6 times higher) in comparison to the caspase-3-FLIP<sub>L</sub> heterodimer.

Complex	r.m.s.d.	Reference
	Å	
Pro-caspase-8-FLIP <sub>L</sub>	0.112	On 53 C $\alpha$ ; PDB file is 1F9E mol B (67)
Caspase-8-FLIP <sub>L</sub>	0.135	On 53 C $\alpha$ ; PDB file is 1F9E mol B (67)
Caspase-3-FLIP <sub>L</sub>	0.776	On 53 C $\alpha$ ; PDB file is 1CP3 mol B (35)

### FIG. 8. Stabilization of the functional active site of caspase-8 in the caspase-8-FLIP<sub>L</sub> hybrid model.

**A**, the activation loop of caspase-8 (in red) is interacting with FLIP<sub>L</sub>. Conformational changes of caspase-8 induced by FLIP<sub>L</sub> allow the formation of the active site of caspase-8. *Top panels* show a general view, whereas a detailed view is shown *below (boxed inset)*. The side chains of residues Asn-407 and Asn-408 of caspase-8 form favorable H-bonds with the side chains Arg-337 and His-396 of FLIP, respectively. This type of interaction, which stabilizes the active conformation of the activation loop, is not present in the active caspase-8 dimer (65). Pro-394 and Thr-337 of caspase-8 are the homologues of His-396 and Arg-337 of FLIP. **B**, processing sites in loop  $\alpha\beta$  of caspase-8 and FLIP. The pro-caspase-8-FLIP heterodimer and the caspase-8 homodimer are shown with a rotation of 90° compared with *panel A*. The Asp residues at the processing sites (in red) are labeled. Loop  $\alpha\beta$  of caspase-8 is shown in dark brown and that of FLIP in light brown. Note that upon cleavage, loop  $\alpha\beta$  of caspase-8 folds over the structure and "locks" the activation loop (shown in red) in the active conformation. The newly generated C terminus at Asp-374 forms a salt bridge with Lys-224 of the second caspase-8. Arg-243 of FLIP may play a role similar to that of Lys-224 of caspase-8.



FLIP<sub>L</sub> revealed good shape complementary surfaces (Fig. 7, A and B). The shape complementarity of the caspase-8-FLIP<sub>L</sub> model was similar to that of pro-caspase-7 (38) (60 and 62%, respectively). It revealed a value of 71%, similar to that observed for the structure of pro-caspase-9 (46) (73%) and of the inhibited caspase-8 (45) (72%) (Fig. 7B). This means that the rearrangement of the caspase-8 active site positively influences the binding of both molecules. Moreover, the electrostatic complementarity in both models was a good fit (Fig. 7C).

The activation loop of caspase-8 comprises 12 residues and is distinct from the  $\alpha\beta$  loop that joins the p18 and p12 subunits.

The activation loop is entirely part of the p12 subunit and comprises one of the Arg residues that normally form the specificity pocket for the P1 Asp residue of the substrate (other residues also form this pocket, but Arg-413 is the one that experiences the largest rearrangement). In the pro-caspase-8 model, the activation loop is positioned in such a way that the active site is not formed. We postulate that, in the pro-caspase-8 homodimer or in the pro-caspase-8-FLIP<sub>L</sub> heterodimer, an active site can form by repositioning of the activation loop, in the absence of any proteolytic processing. This event is unfavorable in a monomer, but is possible in the

pro-caspase-8 homodimer. However, it appears privileged in the pro-caspase-8-FLIP<sub>L</sub> heterodimer, where Asn-407 and Asn-408 in the activation loop of caspase-8 form hydrogen bonds with Arg-337 and His-396 of FLIP<sub>L</sub>, respectively (Fig. 8A). Pro-caspase-8 can, therefore, transiently exist as an active protease, in the absence of processing, and this form is stabilized by FLIP<sub>L</sub>. Active pro-caspase-8 can autoprocess and cleave itself at Asp-374 (and Asp-384). The loop  $\alpha\beta$  appears long enough to fit without major constraints in the active site of pro-caspase-8. In addition, the loop  $\alpha\beta$  of the neighbor FLIP could also be processed, and there is no obvious steric hindrance for this to occur. Once cleaved after Asp-374, the newly generated C terminus of the p18 (or p43) subunit of caspase-8 will fold over the structure, passing over the activation loop and “locking” it in the active conformation (Fig. 8B). In the caspase-8-caspase-8 homodimer, a salt bridge with Lys-224 of the second caspase-8 stabilizes the newly generated C terminus at Asp-374. This explains how caspase-8 can stay in an active conformation, even though the activation loop is not stabilized as efficiently as in the caspase-8-FLIP<sub>L</sub> heterodimer.

In the active, processed caspase-8 complexed with FLIP, Arg-243 of FLIP<sub>L</sub> could play the stabilization role normally played by Lys-224 of caspase-8.

#### DISCUSSION

Although the anti-apoptotic function of FLIP<sub>L</sub> has been well established in the past, it remained an enigma why FLIP<sub>L</sub> also displayed a pro-proapoptotic function upon overexpression. The current report suggests a possible molecular explanation for this phenomenon. Our data are compatible with a model in which FLIP<sub>L</sub> unscrambles the latent proteolytic activity of caspase-8 (Fig. 9). In the caspase-8-FLIP<sub>L</sub> heterodimer, caspase-8 is not released into the cytoplasm because cleavage between the DED and the caspase-unit within caspase-8 and FLIP<sub>L</sub> does not occur. As a result, the activity of the heterodimer remains membrane-restricted and does not result in apoptosis. Only under conditions of non-physiological overexpression of FLIP<sub>L</sub> where high concentrations of FLIP<sub>L</sub> accumulate in the cytoplasm, FLIP<sub>L</sub> can activate non-membrane pro-caspase-8. This causes the activation of caspase-3 or other pro-apoptotic molecules in the cytoplasm, which subsequently leads to apoptosis.

The mechanism of caspase-8 activation through FLIP<sub>L</sub> most likely resembles the one recently proposed for caspase-9 (46). There are two fundamental ways in which protease zymogens are activated, either by limited proteolysis, which removes the peptide that blocks access to the catalytic site, or by co-factor binding, which results in the formation of the active site. Activation by limited processing is required for the downstream caspases-3 and -7, but proteolysis is not only insufficient but also unnecessary for caspase-9. Caspase-9 is suggested to be activated upon dimerization by a “priming” mechanism (46). In this model, the catalytic machinery of the caspase-9 monomer is in an inactive conformation. During dimerization, the activation loop is distorted because of binding to its neighbor and this motion transmits the activation signal to residues surrounding the cysteine in the active site. Structural and biochemical data indicate that only one of the two catalytic sites of the dimer is active, whereas the second caspase-9 remains in its inactive state (46). However, future studies are needed to demonstrate whether the inactive caspase-9 is also present in the apoptosome (60).

This dimerization-induced activation model of caspase-9 would satisfactorily explain our data on caspase-8 activation by FLIP<sub>L</sub>. In analogy with this model, FLIP<sub>L</sub> corresponds to the inactive caspase-9 and induces activation of caspase-8 through allosteric changes occurring upon activation (Figs. 7 and 9). As

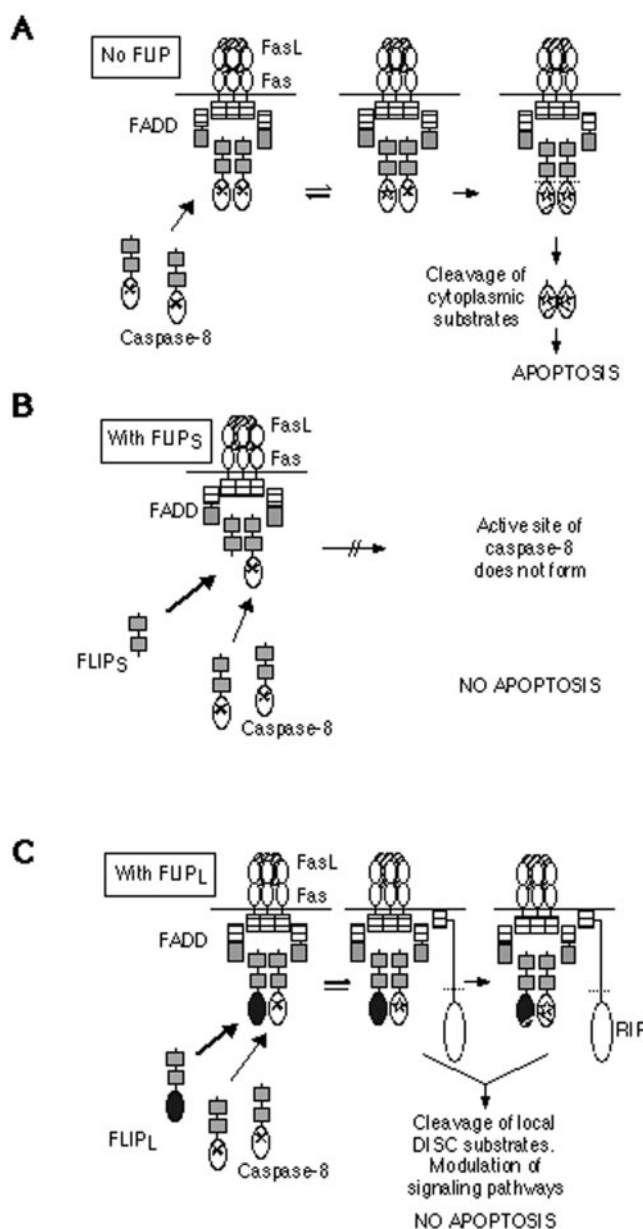


FIG. 9. Proposed mechanism of caspase-8 activation by FLIP. See “Discussion” text for details.

for caspase-9, the interaction between FLIP<sub>L</sub> and caspase-8 is mainly formed by interactions between  $\beta$ -strands. We propose that, under physiological concentrations, the interface interaction is too weak to form heterodimers, and FLIP<sub>L</sub> and caspase-8 remain monomeric in the cytoplasm, whereas heterodimerization is induced upon recruitment to the DISC. Nevertheless, because inhibitor binding stabilizes the active form of caspase-8, heterodimer formation can be artificially induced by adding zVAD-fmk as we show in Fig. 4. Again, this is similar to caspase-9, where inhibitor addition pushes the equilibrium to the dimeric form (46). Thus, the asymmetric caspase-8-FLIP<sub>L</sub> heterodimer has a one-site reactivity, which does not require activation by cleavage, as evidenced by the capacity of non-processed caspase-8 to react with the biotinylated DEVD-aomk substrate.

The activation of precursor caspase-8 is dependent on the caspase-like domain of FLIP<sub>L</sub>. FLIP<sub>S</sub>, which only contains the two DEDs, binds to caspase-8 but is unable to activate it. This short form of FLIP<sub>L</sub> is therefore predicted to act as an inhibitor of FLIP<sub>L</sub> with respect to caspase-8 activation. Indeed, in the

presence of FLIP<sub>S</sub>, co-recruited caspase-8 is unable to cleave the DEVD-aomk substrate. In human primary T cells, FLIP<sub>S</sub> is induced after 3 days of PHA activation (61), predicting that at this time point membrane-bound caspase-8 is inhibited. Indeed, DISC-associated caspase-8 activity inversely correlates with FLIP<sub>S</sub> concentration (62).

What is the target protein of membrane-restricted FLIP<sub>L</sub>-caspase-8 proteolytic activity? It is reasonable to propose that the prime substrate is FLIP itself, which is rapidly cleaved upon stimulation of death receptors. The role of this processing is not known, but cleavage most likely induces a conformational change in FLIP<sub>L</sub>. Cleavage of FLIP<sub>L</sub> may result in a weakening of the interaction between the two proteins, possibly resulting in their dissociation. Alternatively, FLIP<sub>L</sub> cleavage may induce the observed ubiquitination of FLIP<sub>L</sub> and subsequent degradation (63, 64). Yet another possibility is that the cleavage induces conformational changes that are required for the reported association of TRAF family members (27). Experiments with non-cleavable FLIP<sub>L</sub> are currently in progress to test these hypotheses.

The kinase RIP appears to be a second substrate of the FLIP<sub>L</sub>-caspase-8 protease. RIP is known to be crucial for the activation of the transcription factor NF- $\kappa$ B (65). FLIP<sub>L</sub>-caspase-8-induced RIP cleavage leads to the generation of a fragment encompassing the death domain that was previously shown to act as a dominant negative inhibitor of the NF- $\kappa$ B signaling pathway (58). It can therefore be speculated that RIP processing through FLIP<sub>L</sub>-caspase-8 contributes to the down-regulation of the NF- $\kappa$ B signal.

Activation of pro-caspase-8 by FLIP<sub>L</sub> was recently also reported by Chang and colleagues (66). Using an artificial system to induce FLIP<sub>L</sub> dimerization in the cytoplasm, caspase-8 activity was found to be induced. Their interpretation of the results, which are basically in accordance with ours, was that FLIP<sub>L</sub> acted as an inhibitor of caspase-8 only at very high expression levels, whereas at more physiological concentrations, FLIP<sub>L</sub> was required for the activation of caspase-8 and hence for apoptosis. However, this model, although interesting, is difficult to reconcile with the fact that FLIP-deficient cells are highly sensitive to apoptosis (25).

The activity of caspases is tightly controlled to avoid apoptosis. The acquisition of catalytic activity is therefore subjected to severe controls. It appears that different classes of caspases have evolved with distinct ways to acquire catalytic competency. Although downstream caspases are activated by proteolytic cleavage of the activation loop to generate a rearrangement of the active site, at least two upstream caspases (caspase-9 and caspase-8) seem to have opted for an allosteric type of activation without need of limited proteolytic cleavage. This allows activation of the apical caspases in the absence of any activated upstream protease.

**Acknowledgments**—We are grateful to Kimberley Burns for critical reading of the manuscript and the whole Tschopp group for stimulating discussions.

#### REFERENCES

- Jacobson, M. D., Weil, M., and Raff, M. C. (1997) *Cell* **88**, 347–354
- Wolf, B. B., and Green, D. R. (1999) *J. Biol. Chem.* **274**, 20049–20052
- Thornberry, N. A., and Lazebnik, Y. (1998) *Science* **281**, 1312–1316
- Bodmer, J. L., Schneider, P., and Tschopp, J. (2002) *Trends Biochem. Sci.* **27**, 19–26
- Siegel, R. M., Frederiksen, J. K., Zacharias, D. A., Chan, F. K., Johnson, M., Lynch, D., Tsien, R. Y., and Lenardo, M. J. (2000) *Science* **288**, 2354–2357
- Boldin, M. P., Varfolomeev, E. E., Panczer, Z., Mett, I. L., Camonis, J. H., and Wallach, D. (1995) *J. Biol. Chem.* **270**, 7795–7798
- Chinnaiyan, A. M., O'Rourke, K., Tewari, M., and Dixit, V. M. (1995) *Cell* **81**, 505–512
- Medema, J. P., Scaffidi, C., Kischkel, F. C., Shevchenko, A., Mann, M., Krammer, P. H., and Peter, M. E. (1997) *EMBO J.* **16**, 2794–2804
- Kischkel, F. C., Lawrence, D. A., Tinel, A., LeBlanc, H., Virmani, A., Schow, P., Gazdar, A., Blenis, J., Arnott, D., and Ashkenazi, A. (2001) *J. Biol. Chem.* **276**, 46639–46646
- Kischkel, F. C., Hellbardt, S., Behrmann, I., Germer, M., Pawlita, M., Krammer, P. H., and Peter, M. E. (1995) *EMBO J.* **14**, 5579–5588
- Shi, Y. (2002) *Mol. Cell* **9**, 459–470
- Irmeler, M., Thome, M., Hahne, M., Schneider, P., Hofmann, K., Steiner, V., Bodmer, J. L., Schroter, M., Burns, K., Mattmann, C., Rimoldi, D., French, L. E., and Tschopp, J. (1997) *Nature* **388**, 190–195
- Srinivasula, S. M., Ahmad, M., Otilite, S., Bullrich, F., Banks, S., Wang, Y., Fernandes-Alnemri, T., Croce, C. M., Litwack, G., Tomaselli, K. J., Armstrong, R. C., and Alnemri, E. S. (1997) *J. Biol. Chem.* **272**, 18542–18545
- Hu, S., Vincenz, C., Ni, J., Gentz, R., and Dixit, V. M. (1997) *J. Biol. Chem.* **272**, 17255–17257
- Shu, H. B., Halpin, D. R., and Goeddel, D. V. (1997) *Immunity* **6**, 751–763
- Goltsev, Y. V., Kovalenko, A. V., Arnold, E., Varfolomeev, E. E., Brodianskii, V. M., and Wallach, D. (1997) *J. Biol. Chem.* **272**, 19641–19644
- Han, D. K., Chaudhary, P. M., Wright, M. E., Friedman, C., Trask, B. J., Riedel, R. T., Baskin, D. G., Schwartz, S. M., and Hood, L. (1997) *Proc. Natl. Acad. Sci. U. S. A.* **94**, 11333–11338
- Inohara, N., Koseki, T., Hu, Y., Chen, S., and Nunez, G. (1997) *Proc. Natl. Acad. Sci. U. S. A.* **94**, 10717–10722
- Rasper, D., Vaillancourt, J., Hadano, S., Houtzager, V., Seiden, I., Keen, L., Tawa, P., and Nicholson, D. (1998) *Cell Death Diff.* **5**, 271–288
- Thome, M., and Tschopp, J. (2001) *Nat. Rev. Immunol.* **1**, 50–58
- Krueger, A., Baumann, S., Krammer, P. H., and Kirchhoff, S. (2001) *Mol. Cell Biol.* **21**, 8247–8254
- Willems, F., Amraoui, Z., Vanderheyde, N., Verhasselt, V., Aksoy, E., Scaffidi, C., Peter, M. E., Krammer, P. H., and Goldman, M. (2000) *Blood* **95**, 3478–3482
- Krueger, A., Schmitz, I., Baumann, S., Krammer, P. H., and Kirchhoff, S. (2001) *J. Biol. Chem.* **276**, 20633–20640
- Scaffidi, C., Schmitz, I., Krammer, P. H., and Peter, M. E. (1999) *J. Biol. Chem.* **274**, 1541–1548
- Yeh, W. C., Itie, A., Elia, A. J., Ng, M., Shu, H. B., Wakeham, A., Mirtsos, C., Suzuki, N., Bonnard, M., Goeddel, D. V., and Mak, T. W. (2000) *Immunity* **12**, 633–642
- Yeh, W. C., Shahinian, A., Speiser, D., Kraunus, J., Billia, F., Wakeham, A., de la Pompa, J. L., Ferrick, D., Hum, B., Iscove, N., Ohashi, P., Rothe, M., Goeddel, D. V., and Mak, T. W. (1997) *Immunity* **7**, 715–725
- Kataoka, T., Budd, R. C., Holler, N., Thome, M., Martinon, F., Irmeler, M., Burns, K., Hahne, M., Kennedy, N., Kovacsics, M., and Tschopp, J. (2000) *Curr. Biol.* **10**, 640–648
- Lens, S., Kataoka, T., Fortner, K., Tinel, A., Ferrero, I., MacDonald, R. H., Hahne, M., Beermann, F., Attinger, A., Acha-Orbea, H., Budd, R. C., and Tschopp, J. (2002) *Mol. Cell Biol.* **22**, 5419–5433
- Medema, J. P., de Jong, J., van Hall, T., Melief, C. J., and Offringa, R. (1999) *J. Exp. Med.* **190**, 1033–1038
- Djerbi, M., Screpanti, V., Catrina, A. I., Bogen, B., Biberfeld, P., and Grandien, A. (1999) *J. Exp. Med.* **190**, 1025–1032
- Berman, H. M., Westbrook, J., Feng, Z., Gilliland, G., Bhat, T. N., Weissig, H., Shindyalov, I. N., and Bourne, P. E. (2000) *Nucleic Acids Res.* **28**, 235–242
- Okamoto, Y., Anan, H., Nakai, E., Morihira, K., Yonetoku, Y., Kurihara, H., Sakashita, H., Terai, Y., Takeuchi, M., Shibamura, T., and Isomura, Y. (1999) *Chem. Pharm. Bull.* **47**, 11–21
- Rano, T. A., Timkey, T., Peterson, E. P., Rotonda, J., Nicholson, D. W., Becker, J. W., Chapman, K. T., and Thornberry, N. A. (1997) *Chem. Biol.* **4**, 149–155
- Thornberry, N. A., and Molineaux, S. M. (1995) *Protein Sci.* **4**, 3–12
- Mittl, P. R., Di Marco, S., Krebs, J. F., Bai, X., Karanewsky, J. S., Priestle, J. P., Tomaselli, K. J., and Grutter, M. G. (1997) *J. Biol. Chem.* **272**, 6539–6547
- Rotonda, J., Nicholson, D. W., Fazil, K. M., Gallant, M., Gareau, Y., Labelle, M., Peterson, E. P., Rasper, D. M., Ruel, R., Vaillancourt, J. P., Thornberry, N. A., and Becker, J. W. (1996) *Nat. Struct. Biol.* **3**, 619–625
- Lee, D., Long, S. A., Adams, J. L., Chan, G., Vaidya, K. S., Francis, T. A., Kikly, K., Winkler, J. D., Sung, C. M., Debouck, C., Richardson, S., Levy, M. A., DeWolf, W. E., Jr., Keller, P. M., Tomaszek, T., Head, M. S., Ryan, M. D., Heltiwanger, R. C., Liang, P. H., Janson, C. A., McDevitt, P. J., Johanson, K., Concha, N. O., Chan, W., Abdel-Meguid, S. S., Badger, A. M., Lark, M. W., Nadeau, D. P., Suva, L. J., Gowen, M., and Nuttall, M. E. (2000) *J. Biol. Chem.* **275**, 16007–16014
- Riedl, S. J., Fuentes-Prior, P., Renatus, M., Kairies, N., Krapp, S., Huber, R., Salvesen, G. S., and Bode, W. (2001) *Proc. Natl. Acad. Sci. U. S. A.* **98**, 14790–14795
- Wei, Y., Fox, T., Chambers, S. P., Sintchak, J., Coll, J. T., Golec, J. M., Swenson, L., Wilson, K. P., and Charifson, P. S. (2000) *Chem. Biol.* **7**, 423–432
- Huang, Y., Park, Y. C., Rich, R. L., Segal, D., Myszkowski, D. G., and Wu, H. (2001) *Cell* **104**, 781–790
- Chai, J., Wu, Q., Shiozaki, E., Srinivasula, S. M., Alnemri, E. S., and Shi, Y. (2001) *Cell* **107**, 399–407
- Chai, J., Shiozaki, E., Srinivasula, S. M., Wu, Q., Datta, P., Alnemri, E. S., Shi, Y., and Dataa, P. (2001) *Cell* **104**, 769–780
- Blanchard, H., Kodandapani, L., Mittl, P. R., Marco, S. D., Krebs, J. F., Wu, J. C., Tomaselli, K. J., and Grutter, M. G. (1999) *Struct. Fold. Des.* **7**, 1125–1133
- Watt, W., Koepflinger, K. A., Mildner, A. M., Heinrikson, R. L., Tomasselli, A. G., and Watenpaugh, K. D. (1999) *Struct. Fold. Des.* **7**, 1135–1143
- Blanchard, H., Donepudi, M., Tschopp, M., Kodandapani, L., Wu, J. C., and Grutter, M. G. (2000) *J. Mol. Biol.* **302**, 9–16
- Renatus, M., Stennicke, H. R., Scott, F. L., Liddington, R. C., and Salvesen, G. S. (2001) *Proc. Natl. Acad. Sci. U. S. A.* **98**, 14250–14255
- Diederichs, K. (1995) *Proteins* **23**, 187–195
- Kleywegt, G. J., and Jones, T. A. (1998) *Acta Crystallogr. Sect. D Biol. Cryst.*

- tallogr.* **54**, 1119–1131
49. Thompson, J. D., Gibson, T. J., Plewniak, F., Jeanmougin, F., and Higgins, D. G. (1997) *Nucleic Acids Res.* **25**, 4876–4882
50. Sali, A., and Blundell, T. L. (1993) *J. Mol. Biol.* **234**, 779–815
51. Laskowski, R. A., MacArthur, M. W., Moss, D. S., and Thornton, J. M. (1993) *J. Appl. Crystallogr.* **26**, 283–293
52. Lawrence, M. C., and Colman, P. M. (1993) *J. Mol. Biol.* **234**, 946–950
53. Connolly, M. L. (1983) *J. Appl. Crystallogr.* **16**, 548–558
54. Nicholls, A., Sharp, K. A., and Honig, B. (1991) *Proteins* **11**, 281–296
55. Kangas, E., and Tidor, B. (1998) *J. Chem. Phys.* **q09**, 7522–7545
56. Jones, T. A., Zou, J. Y., Cowan, S. W., and Kjeldgaard, M. (1991) *Acta Crystallogr. Sect. A Found. Crystallogr.* **47**, 110–119
57. Roy, S., Bayly, C. L., Garg, Y., Houtzager, V. M., Kargman, S., Keen, S. L., Rowland, K., Seiden, I. M., Thornberry, N. A., and Nicholson, D. W. (2001) *Proc. Natl. Acad. Sci. U. S. A.* **98**, 6132–6137
58. Martinon, F., Holler, N., Richard, C., and Tschopp, J. (2000) *FEBS Lett.* **468**, 134–136
59. Lin, Y., Devin, A., Rodriguez, Y., and Liu, Z. (1999) *Genes Dev.* **13**, 2514–2526
60. Acehan, D., Jiang, X., Morgan, D. G., Heuser, J. E., Wang, X., and Akey, C. W. (2002) *Mol. Cell* **9**, 423–432
61. Holler, N., Zaru, R., Micheau, O., Thome, M., Attinger, A., Valitutti, S., Bodmer, J. L., Schneider, P., Seed, B., and Tschopp, J. (2000) *Nat. Immunol.* **1**, 489–502
62. Kirchhoff, S., Muller, W. W., Li-Weber, M., and Krammer, P. H. (2000) *Eur. J. Immunol.* **30**, 2765–2774
63. Fukazawa, T., Fujiwara, T., Uno, F., Teraishi, F., Kadowaki, Y., Itoshima, T., Takata, Y., Kagawa, S., Roth, J. A., Tschopp, J., and Tanaka, N. (2001) *Oncogene* **20**, 5225–5231
64. Kim, Y., Suh, N., Sporn, M., and Reed, J. C. (2002) *J. Biol. Chem.* **277**, 22320–22329
65. Kelliher, M. A., Grimm, S., Ishida, Y., Kuo, F., Stanger, B. Z., and Leder, P. (1998) *Immunity* **8**, 297–303
66. Chang, D. W., Xing, Z., Pan, Y., Algeciras-Schimmich, A., Barnhart, B. C., Yaish-Ohad, S., Peter, M. E., and Yang, X. (2002) *EMBO J.* **21**, 3704–3714
67. Evans, S. V. (1993) *J. Mol. Graph.* **11**, 127–138